*32nd EPS Conference on Plasma Phys. Tarragona, 27 June - 1 July 2005 ECA Vol.**29C**, P-2.061 (2005)*

Locked mode thresholds on the MAST spherical tokamak

D.F. Howell[1], T.C. Hender[1], G. Cunningham[1], R.J. La Haye[2], J.T. Scoville[2]

[1] *EURATOM/UKAEA Fusion Association, Culham Science Centre, Abingdon, Oxon, OX14 3DB, UK*

[2] *General Atomics, PO Box 85608, San Diego, CA, 92186-5608, USA*

Introduction

In an ideal tokamak, the equilibrium magnetic fields would be axisymmetric. In practice, however, the magnetic fields show small deviations from axisymmetry which are known as error fields. It is well known that error fields with amplitudes $B_r/B_T \sim 10^{-4}$, where B_T is the toroidal field at the geometric axis, can induce non-rotating, or locked, resistive tearing modes in the plasma[1]. These locked modes typically lead to termination of the plasma.

To reduce the effect of these error fields, a set of error field correction coils has been installed on the MAST tokamak. These are designed to create non-axisymmetric magnetic fields inside the machine to oppose the intrinsic error field. Correction of the intrinsic error field has allowed MAST to operate in previously inaccessible regimes.

Experiments have been carried out to measure the locked mode threshold by applying large error fields using the coils. In this way we have determined how the locked mode threshold scales with density, q and toroidal field.

The MAST error field correction coils

The MAST error field correction system consists of four coils attached to the outside of the vessel as shown in Figure 1. In the experiments described here, opposite pairs of coils were wired in series to produce a predominantly $n = 1$ spectrum. The two pairs of coils are powered by independent power supplies. This enables us to apply an $n = 1$ field at an arbitrary toroidal phase. The two pairs of coils are labelled 'EFC A' and 'EFC B' in this paper.

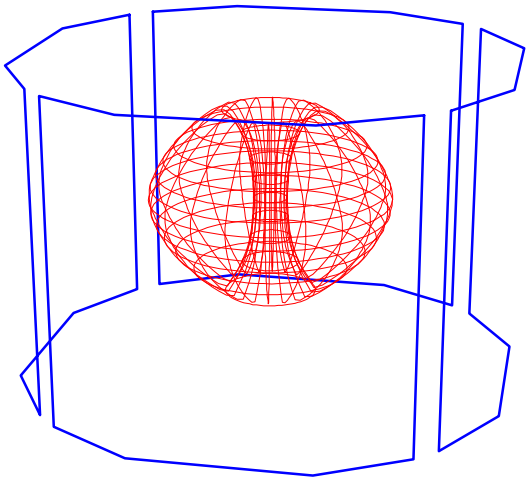

Figure 1: The MAST error field coils

Experimental technique

In the experiments performed on MAST, the following procedure was adopted. Firstly a steady state Ohmic, L mode, double null plasma with a given toroidal field, plasma current and density is formed. The current in one of the error field coils is then ramped up until a locked

mode is formed, see Figure 2. These locked modes have no rotating $m = 2$, $n = 1$ precursor mode.

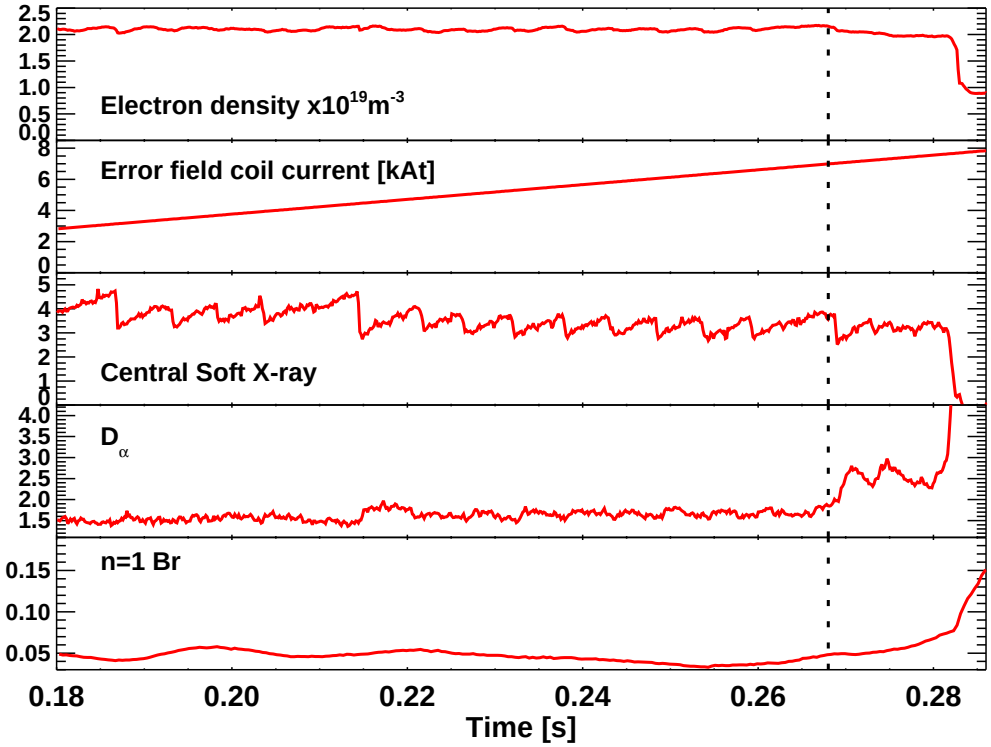

Figure 2: Time traces for a typical shot. The onset of the locked mode is indicated by a sudden drop in the electron density, the disappearance of the sawteeth and a rise in the D_α emission at the divertor.

This procedure is performed for positive and negative currents in the two sets of error field coils. These currents are plotted in Figure 3 and can be seen to lie on a circle. The radius of this circle is related to the amplitude of applied field required to form the locked mode, and the centre of the circle is identified as giving the error field currents which will best minimise the intrinsic error of the machine.

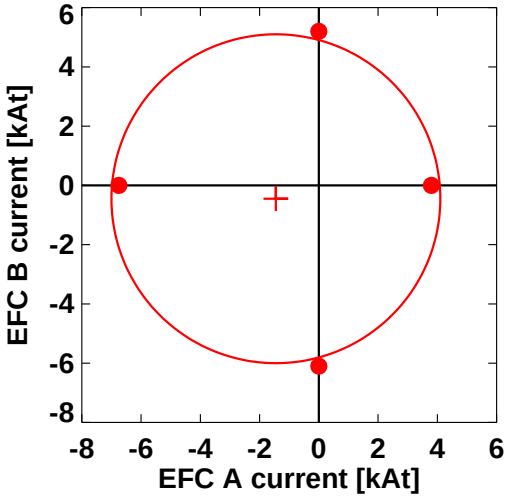

Figure 3: The currents required to induce a locked mode lie on a circle.

Error field correction

Error field correction has allowed access to operating regimes which were otherwise unattainable. By applying the currents in the error field correction coils corresponding to the centre of the circle in Figure 3 it was possible to achieve a density 30% lower than that achievable otherwise, as shown in Figure 4. It can be seen that in the case where there was no error field

correction, blue traces, a locked mode starts to grow from 210ms. We see a sudden drop in density, the sawteeth disappear and the discharge disrupts at 260ms. With error field correction, red traces, the discharge is seen to continue dropping in density, no locked mode is seen and the discharge runs to full length.

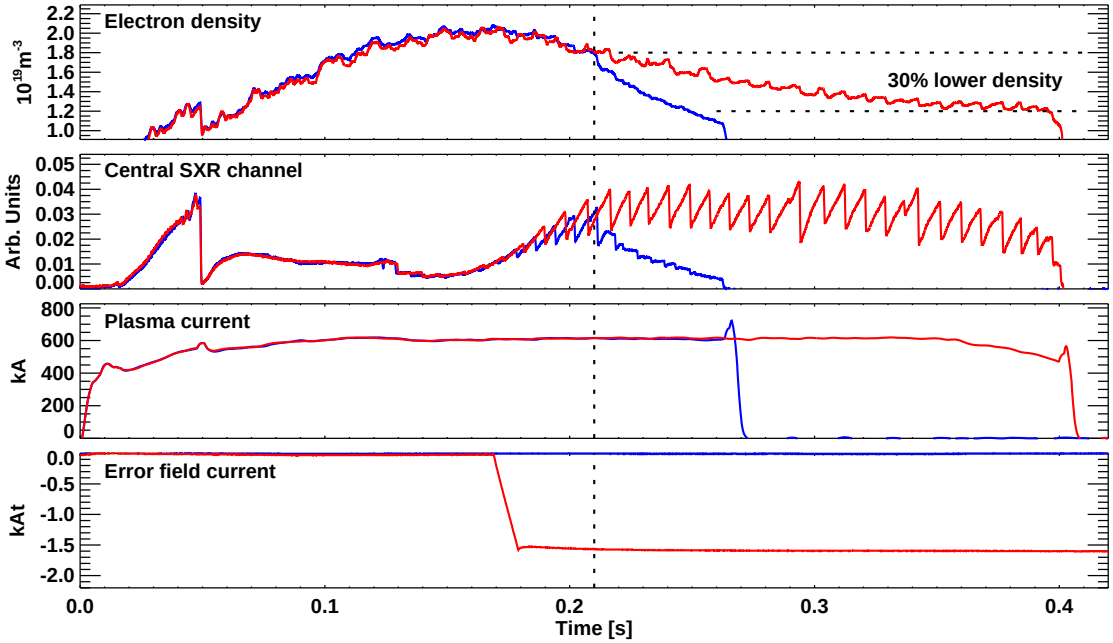

Figure 4: Time traces for shots with (red) and without (blue) error field correction.

Locked mode threshold scalings

Figure 5 shows the results of scans that were performed in order to determine how the locked mode threshold scales with density, toroidal field and q. The density scan, Figure 5a, was performed at fixed $B_T = 0.55T, I_p = 600kA$. The open point had a different value of q_{95} than the rest of the dataset and so was not included in the fit. The toroidal field scan, Figure 5b, was performed at fixed density, $n_e = 2.3x10^{19}m^{-3}$ with the ratio B_T/I_p fixed. The q scan, Figure 5c, was performed at fixed density, $n_e = 2.2x10^{19}m^{-3}$ and $B_T = 0.6T$. Here the scaling is presented as a function of the cylindrical q

$$q_{cyl} = \frac{5000a^2B_T}{I_pR_{geom}}$$

where a is the minor radius in m, I_p is the plasma current in kA, B_T is the toroidal field in T at the geometric radius, R_{geom} which is in m. The full scaling is represented as a power law

$$\frac{B_{21}}{B_T} \sim n_e^{1.1\pm0.17}B_T^{-0.69\pm0.11}q_{cyl}^{1.36\pm0.16}$$

Here, B_{21} is the $m = 2$, $n = 1$ component of the applied radial magnetic field at the $q = 2$ surface. Also shown in Figure 5 is a comparison of the exponents, α_n, α_B and α_q in the power

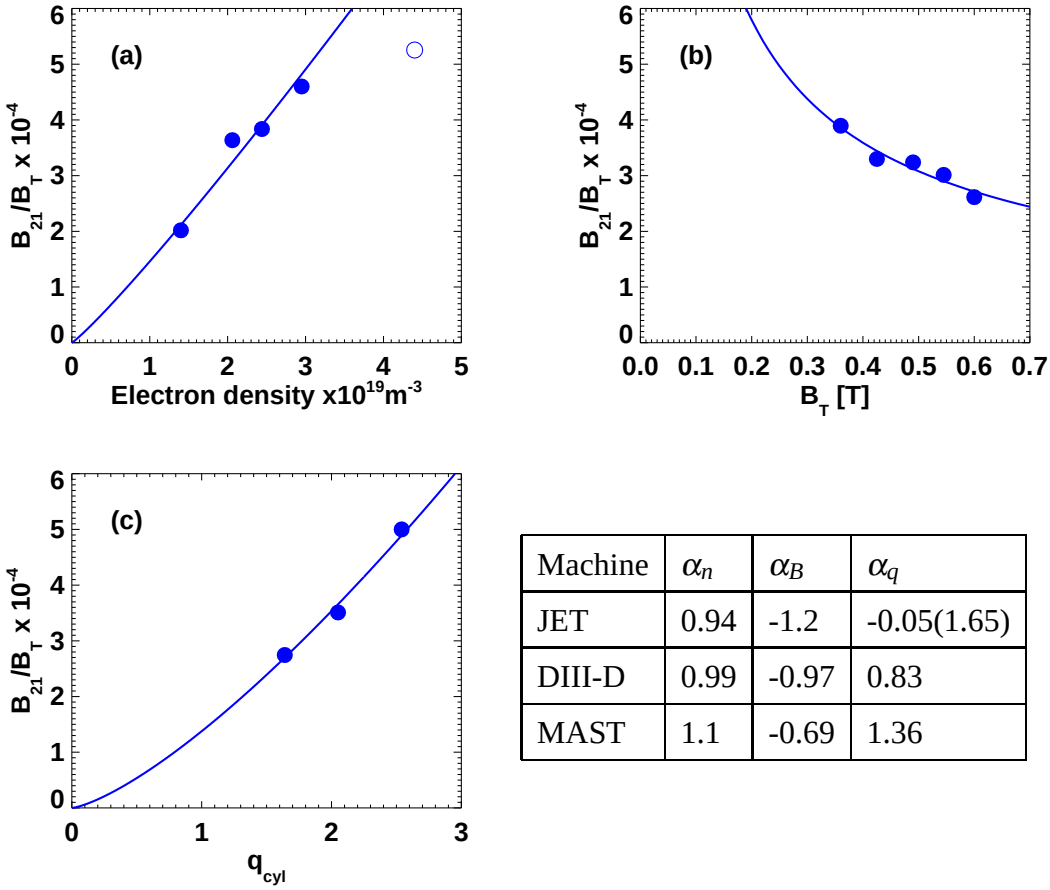

Machine	α_n	α_B	α_q
JET	0.94	-1.2	-0.05(1.65)
DIII-D	0.99	-0.97	0.83
MAST	1.1	-0.69	1.36

Figure 5: Scaling of the locked mode threshold with density, toroidal field and q_{cyl}.

law fit for MAST, DIII-D and JET[1]. The second JET figure for the α_q scaling was obtained from experiments using the new external correction coils, which have a better match in harmonic spectrum to the MAST and DIII-D coils than the older saddle coils. We see that the density scaling is approximately linear for all three machines and that the toroidal field and q scalings, whilst showing some variation, are broadly in line with each other.

In summary, these results extend the range of machines over which error field scalings have been studied to include low aspect ratio, and comparisons with DIII-D which has an equivalent poloidal cross-section are in progress to elucidate any aspect ratio effects.

This work was funded jointly by the United Kingdom Engineering and Physical Sciences Research Council and by the European Communities under the contract of Association between EURATOM and UKAEA. The views and opinions expressed herein do not necessarily reflect those of the European Commission.

References

[1] ITER physics basis editors, Nuclear Fusion **39**, pp. 2286-2294 (1999)